A highly selective and sensitive competitive aptasensor capable of quantifying thrombin elevated with side effects in severe COVID-19

Jaden Yun [a,b], Ji Hoon Lee [a,*]

[a] Luminescent MD, LLC, Hagerstown, MD 21742, United States
[b] Phillips Exeter Academy, Exeter, NH 03833, United States

ABSTRACT

To protect critical injury from blood clots with side effects in severe COVID-19, a highly selective and sensitive biosensor was developed for the quantification of trace levels of thrombin using the combination of a DNA aptamer (TBA) of thrombin and a complementary strand of TBA. TBA rapidly binds with thrombin, whereas it slowly binds with the complementary strand to form a double stranded DNA (dsDNA). SFC green intercalated into dsDNA cannot emit light in 1,1′-oxalyldiimidazole chemiluminescence (ODI-CL) reaction because high-energy intermediates formed from ODI-CL reaction cannot transfer energy to SFC trapped in dsDNA. However, SFC freely existing with the formation of G-quadruplex from the reaction of thrombin and TBA emits bright chemiluminescence because the high-energy intermediates can transfer energy to SFC (or camel) in solution. Thus, the brightness of light emitted in ODI-CL reaction was proportionally enhanced with the increase of thrombin in a sample due to the increase of G-quadruplex and reduction of dsDNA. The limit of detection (LOD) of the label free aptasensor operated with good linear calibration curve (10–320 mU/ml) was as low as 3 mU/ml (or 43 pM). Also, the biosensor was quantified trace levels of thrombin with good accuracy, precision, and reliability.

1. Introduction

Recently, it was reported that patients hospitalized with severe COVID-19 infections have high levels of the blood clotting protein factor V [1]. The results indicate that the patients are at elevated risk for blood clots because prothrombin can be rapidly converted into thrombin, known as a coagulation factor, with the increase of the factor V. Thrombin can convert fibrinogen into clottable fibrin in the hemostasis process as shown in Scheme S1. Thus, it is important to develop a biosensor capable of monitoring the activity of thrombin to protect critical injury from blood clots. This is because the accurate monitoring of thrombin in blood can provide information to decide whether patients need to be treated with antithrombotic agents [2,3].

After the developments of aptamers using peptides and RNAs in 1990 [4,5], nucleic acid aptamers selected from a large pool of random sequences were also designed and synthesized to quantify target molecules in a sample collected from human, food, and nature [6]. For example, 15nt thrombin aptamer (TBA,5′-GGTTGGTGTGGTTGG-3′) developed to inhibit thrombin activity in human blood has been widely applied as a capturing material of in-vitro biosensors for the monitoring of thrombin

activity in human blood [6]. As shown in Fig. 1(A), a guanine (G)-quadruplex is formed when TBA binds to one of two anion binding recognition exosites of thrombin, the fibrinogen-recognition exosite, with a dissociation constant (Kd) of ~ 100 nM as shown in Fig. 1(A) [7–9]. The two square planar structures of G-quadruplex were formed through the hydrogen bonding between guanines as shown in Fig. 1(B) [7].

1,1′-Oxalyldiimidazole chemiluminescence (ODI-CL) is generated with the chemiluminescence resonance energy transfer (CRET) between fluorescence dye and high-energy intermediate (**X**) formed from the reaction of ODI and H_2O_2 as shown in Scheme 1 [10–12]. **X** acts like a light source, such as LED, Laser, and Xenon, of fluorescence spectrometer. Thus, the emission wavelength of the light emitted from a fluorescence dye in ODI-CL reaction is similar to that of the fluorescence dye [12]. Using the chemical and physical properties of ODI-CL, it, instead of fluorescence, was applied as a highly sensitive detection method to analyze trace levels of biological, environmental, or toxic material in a sample [13–16]. The reports noted that ODI-CL is much more sensitive than fluorescence. Scheme S2 shows possible chemical structures of **X**. The efficiency of **X** for the CRET were dependent on structures of ODI

derivatives [11,12]. For example, it was reported that **X** formed from the reaction between 1,1′-oxalyldi-4-methylimidazole (OD4MI) and H_2O_2 is the strongest for the CRET to emit bright CL [11].

TBA composed of the single stranded DNA (ssDNA) can be formed as a double stranded DNA (dsDNA) when it binds with a complementary strand (5′-CCAACCACACCAACC-3′). In general, the concentration of dsDNA formed from the hybridization between TBA and the complementary strand can be determined using dsDNA quantification kits operated with fluorescence detection. This is because dyes used in the dsDNA quantification kit emits bright fluorescence when they intercalate to specific sequences in the minor groove of dsDNA [17,18]. In other words, free dyes existing in the absence of dsDNA emit very weak fluorescence, whereas dyes intercalated in the minor groove of dsDNA emit bright fluorescence.

Based on the Fig. 1, Scheme 1, and the role of dsDNA quantification kits, we expected that a highly selective and sensitive aptasensor with ODI-CL detection can be designed and developed for the monitoring of thrombin in a sample. We confirmed in this research that the label free aptasensor can be applied for monitoring the activity of thrombin to prevent critical injury from blood clots. Details are described below.

2. Materials and methods

2.1. Chemicals and materials

TBA and the complementary strand of TBA were purchased from Alpha DNA (Montreal, Canada). Calf thymus dsDNA and thrombin (100 Unit, 50 μg, mol wt.: 34.7 kDa) were purchased from Sigma Aldrich (Milwaukee, IL, USA) Sunfine Global provided Sun-Fine-Chem (SFC) green and camel green for the research (Cheongju, South Korea). Bis (2,4,6-trichlorophenyl) oxalate (TPCO) and 4-Methylimidazole were purchased from TCI America (Portland, OR, USA). 4′,6-Diamidine-2′-phenylindole dihydrochloride (DAPI), bisBenzimide H 33258 (Hoechst 33258), and bisBenzimide H 33342 trihydrochloride (Hoechst 33342) were purchased from Cayman Chemicals (Ann Arbor, MI, USA). Fluorogenic substrate (Benzoyl-Phe-Val-Arg-AMC, HCl, 25 mg) of thrombin was purchased from Sigma-Aldrich (Saint Louis, MO, USA). Additional buffers and chemicals (ACS grade) used in this research were purchased from VWR (Radnor, PA, USA). Several types of coagulation factors (e.g., thrombin, Va, Xa) and proteins (e.g., prothrombin, V, fibrinogen) were purchased from Prolytix (Essex Junction, VT, USA). Human serum samples were purchased from Innovative Research (Novi, MI, USA).

2.2. Methods

2.2.1. Measurement of fluorescence and ODI-CL after the reaction between SFC green and calf thymus dsDNA

The stock solution (10 mM) of SFC green provided from Sunfine Global was 2000-fold diluted in Tris-HCl buffer solution (pH 8.5, 10 mM). The working solution (5 μM, 100 μl) was mixed with a certain concentration of dsDNA (100 μl) in a well of 96-wellplate. The mixture was incubated for 2 min for the intercalating reaction between SFC green and dsDNA. Sunfine Global noted that SFC green binds primarily with CG sequences in the minor groove of dsDNA.

After the reaction, fluorescence intensity of each sample was measured at 516 nm (excitation wavelength: 493 nm) with a microplate reader with fluorescence detection (Infinite M 1000 of Tecan, Inc. San Jose, CA, USA).

Also, the sample (10 μl) in the 96-wellplate was transferred into a borosilicate test tube to measure bright CL emission based on the reaction pathway shown in Fig. 2(B). The test tube was inserted into a luminometer with two syringe pumps (Lumat 9507, Berthold, Inc., Oak Ridge, TN, USA). Then, H_2O_2 (25 μl) and OD4MI (25 μl) formed from the reaction of TCPO and 4-methylimidazole [11] were consecutively injected into the test tube through the two syringe pumps. With the injection of ODI, green chemiluminescence was immediately generated. The luminometer measured the brightness of chemiluminescence for 2 s. The image of ODI-CL emitted in a well of 96-wellplate was obtained using the functions of a smartphone (LG V30, Gaithersburg, MD, USA) capable of integrating the emission for 30 s

2.2.2. Hybridization of TBA and complementary strand

TBA and the complementary strand were prepared in in Tris-HCl buffer (60 mM, pH 8.5). A certain concentration of TBA (100 μl) was mixed with excess complementary strand (3 μM, 100 μl) in a 1.5-ml microcentrifuge tube. Each sample put into a shaker (Eppendorf Thermomixer, Enfield, CT, USA) was incubated for 3 h for the hybridization at 45 °C. After the incubation, a certain concentration of SFC green was added to the microcentrifuge tube to measure fluorescence and chemiluminescence.

2.2.3. Competitive reaction of thrombin and the complementary strand in the presence of TBA

The solution (100 μl) containing a certain concentration of thrombin and 1 μM TBA was mixed with the complementary strand (3 μM, 100 μl) in a 1.5-ml microcentrifuge tube. The mixture was incubated for 3 h at 45 °C in the shaker. After the incubation, the mixture was cooled at ambient condition. Then, 10 μM SFC Green (50 μl in Tris-HCl buffer, pH 8.5) was added in the mixture (50 μl) containing G-quadruplex TBA aptamer bound with thrombin and dsDNA formed from the
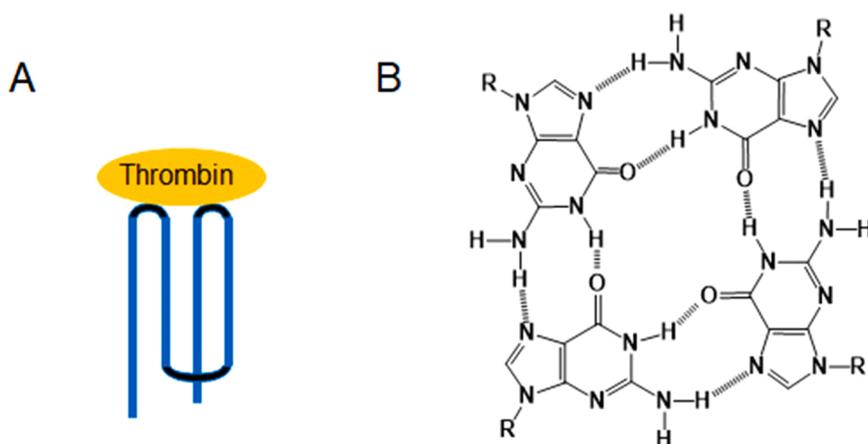
Fig. 1. (a) G-quadruplex TBA aptamer bound with thrombin, (b) G-tetrad structure of guanines in G-quadruplex TBA.

hybridization. The final solution was incubated for 2 min at room temperature (21 ± 2 °C) for the intercalating interaction between dsDNA and SFC Green.

2.2.4. ODI-CL measurement of samples prepared with the competitive reaction

The final products formed from the competitive reaction occurred in the presence of a standard (or sample) emitted chemiluminescence with the addition of ODI-CL reagents. In other words, after the intercalating reaction of SFC (or camel green) and dsDNA in the absence or presence of the standard (or sample), the relative CL intensity was measured with the addition of H_2O_2 and ODI. The relative CL intensify emitted from each sample was measured with the luminometer with two syringe pumps.

2.2.5. Recovery test of the new biosensor capable of quantifying TBA

A certain concentration of TBA was spiked in 10 % human serum. The sample (50 μl) was mixed with 1 μM TBA (50 μl). Then, the complementary strand (3 μM, 100 μl) was added in the mixture (100 μl). The final solution in a 1.5-ml microcentrifuge tube was incubated for 3 h at 45 °C. The concentration of thrombin in each sample after the competitive reaction was determined with the aptasensor with ODI-CL detection. In order to determine the recovery for each sample, the concentration of thrombin quantified with the competitive aptasensor was compared with the thrombin concentration spiked in the sample.

2.2.6. Correlation of the aptasensor with ODI-CL detection and the protease enzyme assay with fluorescence detection

The correlation between the competitive aptasensor with ODI-CL detection and a commercially available protease enzyme assay with fluorescence detection was studied with 10 % human serum containing a certain concentration of thrombin. First, thrombin in each sample was quantified with the calibration curve (10 – 320 mU/ml) of the competitive aptasensor with ODI-CL detection. In order to quantify the concentration of thrombin in each sample using the protease enzyme assay, the sample (50 μl) was added into a well of a 96 well plate (black). Then, fluorogenic substrate (50 μl, 5 μg/ml) of thrombin (Benzoyl-Phe-Val-Arg-AMC) in Tris-HCl buffer (pH 8.5) was injected into the well. The mixture was incubated for 10 min at room temperature. After the incubation, fluorescence intensity of AMC (excitation: 360 nm, emission: 460 nm) emitted in each well was measured with a microplate reader with fluorescence detection (Infinite M 1000 of Tecan, Inc.). The concentration of thrombin in each sample was determined with a linear calibration curve (3.6 – 690 mU/ml) of the protease enzyme assay. Fig. S1 shows the brief procedure of protease enzyme assay with fluorescence detection. As shown in Fig. S1(B), the fluorogenic substrate cannot emit fluorescence in the absence of protease, such as thrombin, due to the fluorescence resonance energy transfer (FRET) between the fluorescence dye and the quencher. However, fluorescence dye separated from the hydrolysis reaction between the fluorogenic substrate and the protease can emit fluorescence as shown in Fig. S1(C). Thus,

fluorescence intensity is enhanced with the increase of protease concentration. Benzoyl and AMC in the fluorogenic substrate of thrombin are a quencher and a fluorescence dye.

3. Results and discussion

3.1. Similarity and difference between ODI-CL and fluorescence in the presence of dsDNA and SFC green (or Camel green)

SFC green emits green chemiluminescence (CL) as well as fluorescence shown in Fig. 2(A). The emission wavelength (528 nm) of SFC green in ODI-CL reaction was slightly longer than the fluorescence wavelength (523 nm) of SFC as chemiluminescence and fluorescence spectra shown in Figs. S2 and S3. The result is consistent with the previous report that emission wavelength of fluorescence dye in ODI-CL reaction was red-shifted because the properties of the high-energy intermediate, **X**, formed from ODI-CL reaction is different from those of light sources of fluorescence spectrometer [12]. As shown in Fig. 2(A), in addition, free SFC green emits bright green light in ODI-CL reaction, whereas it emits very weak green fluorescence. These results indicate that the physical property of **X** formed from the reaction ODI and H_2O_2 is completely different from that of laser (or Xenon lamp) even though they are applied as a light source. The results indicate that a dye (e.g., SFC green, camel green) having low fluorescence quantum efficiency can emit bright chemiluminescence after the rapid CRET between the dye and X. Fig. 2(B) shows the possible ODI-CL reaction mechanism in the presence of SFC green. The trends of ODI-CL emitted from camel green were the same as those generated from SFC green because they are just emitters in ODI-CL reaction (Data not shown).

The relative CL intensity was exponentially dropped down with the increase of calf thymus dsDNA, whereas fluorescence was enhanced as shown in Fig. 2(A) and (C). Fig. 2(C) shows that the shape of CL spectrum in the absence of dsDNA is the same as that in the presence of dsDNA. For example, the time (0.4 s) necessary for attaining the maximum CL intensity (I_{max}) observed under the two different conditions was the same. The results indicate that CL spectra in the absence and presence of calf thymus dsDNA were from free SFC green. In addition, these results indicate that the SFC green (or camel green) captured in the minor groove of dsDNA cannot receive energy from **X** due to the shielding effect of dsDNA even though SFC green bound with specific sequences of dsDNA emitted enhanced fluorescence at 523 nm when it was excited at 493 nm. Also, Fig. 2(A) shows that fluorescence quantum efficiency of SFC green bound with a specific sequence of dsDNA is higher than that of free SFC green.

Based on the experimental results shown in Fig. 2, we confirmed that SFC green can be used as a new dye capable of quantifying dsDNA using a fluorescence sensor. Also, we expected that ODI-CL can be applied as a novel biosensor for the rapid quantification of dsDNA based on the trend shown in Fig. 2.
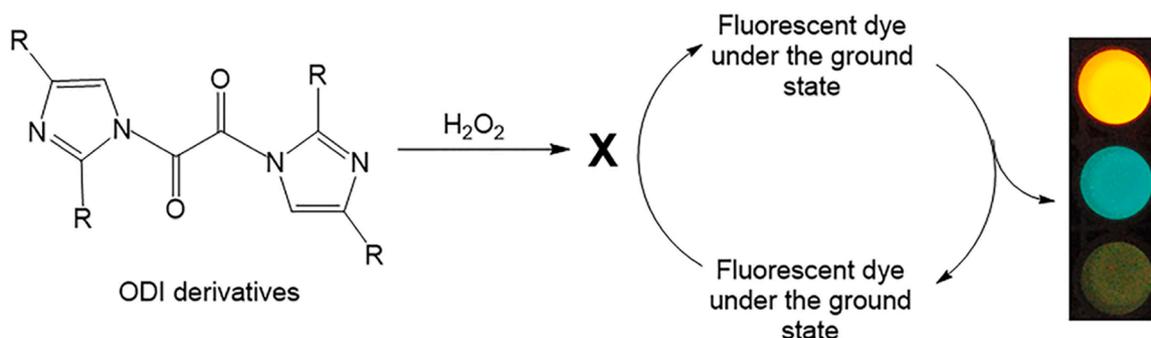
Scheme 1. ODI-CL reaction mechanism. R is H, CH_3 or CH_2CH_3. X is a high-energy intermediate formed from the reaction of ODI and H_2O_2.
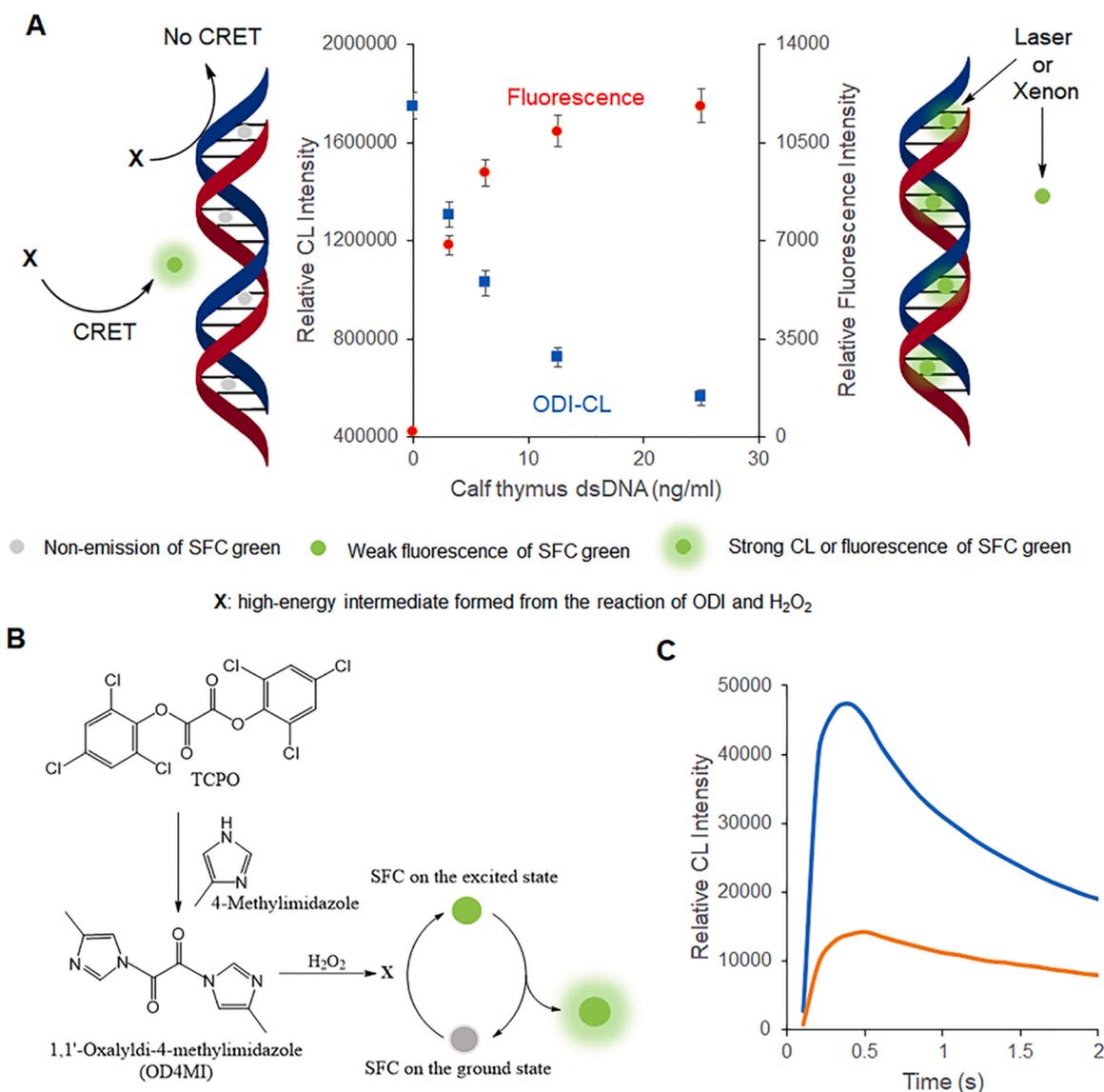
Fig. 2. . (A) Similarity and difference of ODI-CL and fluorescence in the presence of calf thymus dsDNA and SFC green, (B) Possible ODI-CL reaction mechanism in the presence of SFC green, (C) ODI-CL spectra in the absence and presence of calf thymus dsDNA.

3.2. Understanding and optimization of variables to devise a highly sensitive biosensor with ODI-CL detection capable of rapidly sensing dsDNA in a sample

As shown in Fig. 3(A), SFC green immediately reacts with calf thymus dsDNA (15 ng/ml). The relative CL intensity (CL) in the presence of dsDNA was lower than 30 % of the relative CL intensity (CL_0) in the absence of dsDNA. CL/CL_0 measured immediately after mixing SFC green (5 µM) and dsDNA was the same as those measured after incubating for a certain time period within the statistically acceptable error range (< 5 %) as shown in Fig. 3(A). The results indicate that it is possible to devise a biosensor capable of rapidly quantifying dsDNA in a sample using ODI-CL detection.

Fig. 3(B) shows that the relative CL intensity was constant in the presence of different single-stranded DNA (ssDNA) concentrations because SFC green does not interact with ssDNA. The result indicates that it is possible to develop a biosensor capable of sensing dsDNA with good specificity.

Fig. 3(C) shows that CL/CL_0 depends on the concentration of SFC green. CL/CL_0 determined in the presence of 4000-fold diluted SFC green (2.5 µM) with the stock solution was the lowest. The result

indicates that the best concentration of SFC green to quantify trace levels of dsDNA is as low as 2.5 µM.

Commercially available kits capable of quantifying dsDNA contains Tris-EDTA (TE) buffer solution with fluorescence detection. Thus, we prepared two different TE buffers at pH 8 and 8.5. Each TE buffer solution contains 10 mM Tris-HCl and 1 mM EDTA. Also, 10 mM Tris-HCl (pH 8.5) was prepared to select the best buffer solution to develop a highly sensitive biosensor with ODI-CL detection. As shown in Fig. 3(D), CL/CL_0 in Tris-HCl buffer was lower than those in the rest buffer solutions. Thus, Tris-HCl buffer was selected for the research. Based on the results shown in Fig. 3(D), pH effect of Tris-HCl buffer solution was studied. Fig. 2(E) indicates that the best pH is 8.5 to analyze trace levels of dsDNA in a sample.

Fig. 3(F) shows that CL/CL_0 determined with SFC green was lower than those obtained with other dyes widely applied to quantify dsDNA. The result indicates that the biosensor operated with SFC green can rapidly quantify trace levels of dsDNA in a sample. Also, camel green is also a suitable candidate for the development of a biosensor because CL/CL_0 in the presence of camel green is slightly higher than that in the presence of SFC green. CL_0 of camel green was about 2-fold higher than that of SFC green. However, DAPI may not be an appropriate candidate
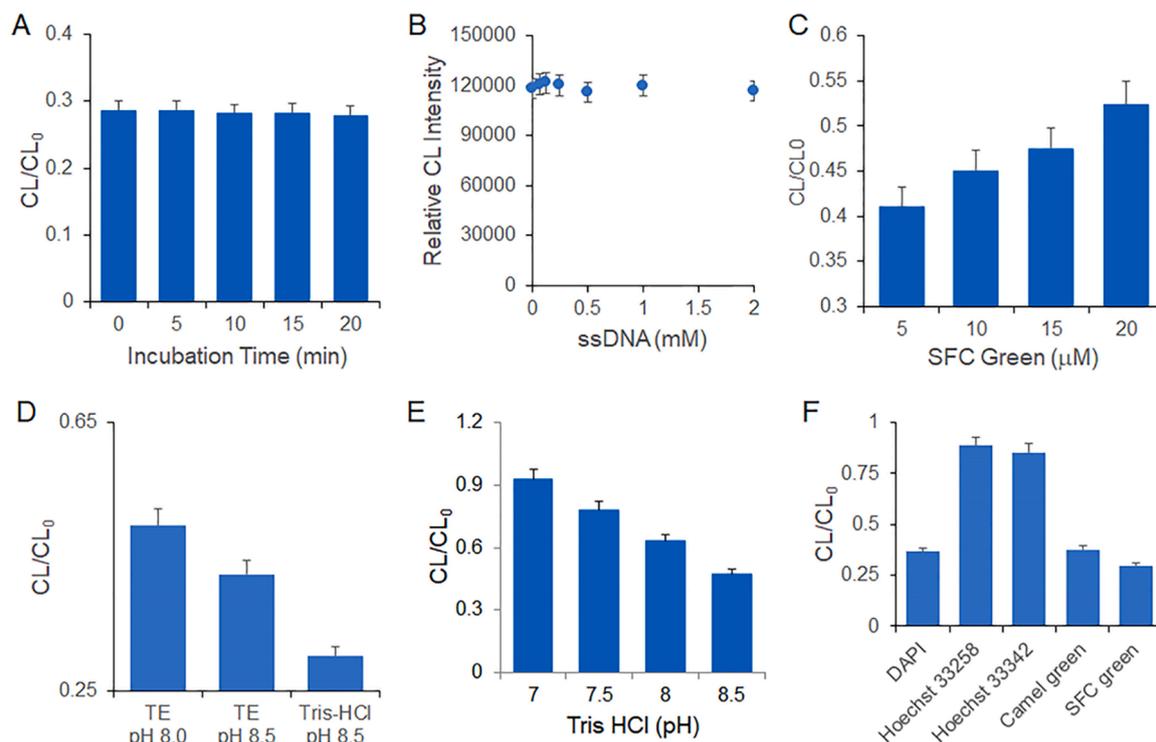
Fig. 3. . (A) Effect of incubation time for the reaction of SFC green and calf thymus dsDNA, (B) Relative CL intensity of SFC green in the presence of ssDNA, (C) Effect of SFC green concentration in the presence of calf thymus dsDNA, (D) Selection of buffer solution for the reaction of SFC green and calf thymus dsDNA, (E) pH effect of Tris-HCl for the reaction of SFC green and dsDNA, (F) Comparison of various dyes applied to quantify dsDNA using ODI-CL detection.

as a dye of a biosensor with ODI-CL detection even though the CL/CL_0 of DAPI is as low as that of camel green. This is because CL_0 of DAPI is too low to quantify trace levels of dsDNA with good accuracy, precision, and reproducibility. CL_0 of DAPI was about 27-fold lower than that of SFC green. Also, CL_0 of DAPI was only 4.5-fold higher than the background measured in the absence of a dye such as DAPI, camel green, and SFC green.

3.3. Hybridization of TBA and complementary strand

Fig. 4(A) shows that dsDNA molecules are formed from the hybridization between TBA and the complementary strand. The relative CL intensity after the hybridization reaction was lower than that in the presence of TBA only due to the intercalating interaction between SFC green and dsDNA. Thus, we observed that CL image in TBA only was

brighter than that in the presence of dsDNA molecules formed from the hybridization. The results are consistent with those confirmed with SFC green and calf thymus dsDNA shown in Fig. 2.

Fig. 4(B) shows that the concentration of dsDNA formed from the hybridization depends on the temperature for hybridization reaction. Based on the results shown in Fig. 4(B), all hybridization reactions of TBA and TBA complementary strand were processed at 45 °C to enhance the yield of dsDNA. We expect that the aptasensor operated at 45 °C is more sensitive than that generated at room temperature or 37 °C because free TBA concentration can be rapidly hybridized with the complementary strand at 45 °C.
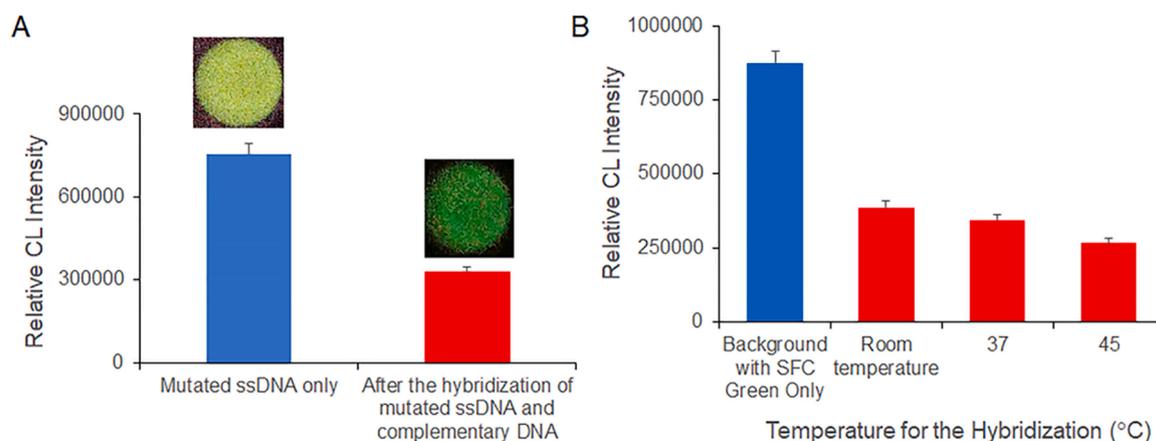
Fig. 4. . (A) Relative CL intensities measured before and after the hybridization of TBA and the complementary strand, (B) Effect of temperature on the hybridization.

3.4. Design of a competitive aptasensor operated with the binding reaction of thrombin and TBA as well as the hybridization of TBA and the complementary strand

Based on the preliminary experimental results shown in Figs. 3 and 4, we designed a competitive aptasensor as shown in Fig. 5(A). First, TBA binds with thrombin existing in a sample as well as hybrids with the complementary strand for 3 h at 45 °C. Then, 10 μM SFC green is added in the solution. The mixture was incubated for 2 min to complete the intercalating interaction between SFC green and dsDNA at room temperature. After the final incubation, the brightness of solution emitted with the addition of ODI-CL reagents was dependent on the concentration of thrombin in human serum.

In order to develop a highly sensitive competitive aptasensor, we studied whether CL emission of SFC green is dependent on the concentration of human serum containing thrombin. As shown in Fig. 5(B), the brightness of SFC emitted in ODI-CL reaction was constant within a statistically acceptable error range (± 3 %).

Graugnard and his collaborators reported the hybridization of DNA (or RNA) in 50 % human serum was slightly faster than that in hybridization buffer only [19]. Based on the results of Fig. 5(B) and the report [19], it is possible that thrombin existing in at least 50 % human serum can be quantified with a competitive aptasensor shown in Fig. 5 (A).

Unfortunately, however, Fig. 5(C) indicates that the binding rate of thrombin and TBA is decreased with the increase of human serum percent (%) concentration containing 300 mU/ml thrombin. The results are consistent with that reported by Cho and her collaborators [7]. As shown in Fig. 5(C), CL/CL_0 in the presence of 10 % human serum was about 14 % lower than that in Tris-HCl buffer. CL/CL_0 in the presence of 40 % human serum was only 1.08. Based on the results, we developed a competitive aptasensor for the quantification of thrombin in 10 % human serum.

As shown in Fig. 5(D), CL emission of SFC (or camel) green in the presence of thrombin in 10 % human serum was stronger than that in the absence of thrombin. This is because the number of dsDNA formed from the hybridization of TBA and the complementary strand is decrease in the presence of thrombin based on the operational procedure of the competitive aptasensor shown in Fig. 5(A). In other words, the CL emission was enhanced because the concentration of free SFC (camel) green was increased with the formation of the G-quadruplex from the interaction of thrombin and TBA. In addition, Fig. 5(A) indicates that the CL emission ratio of SFC green in presence of thrombin is larger than that of camel green.

Based on the results shown in Fig. 5, we designed the competitive aptasensor operated with SFC green for the quantification and monitoring of thrombin in 10 % human serum.

3.5. Quantification of thrombin and recovery test

As shown in Fig. S4, we confirmed that the competitive aptasensor with ODI-CL detection can quantify trace-levels of thrombin in a sample using the calibration curve with the good linearity. The dynamic range of calibration curve was 10–320 mU/ml (or 0.14–4.61 nM). The limit of detection (LOD = 3 S/slope) was as low as 3 mU/ml (or 43 pM). S is a standard deviation determined by measuring the background 20 times. As shown in Table 1, LOD of the biosensor is similar to, lower or higher than those of other biosensors developed with TBA and various detections such as chemiluminescence [18,19], colorimetric [20], electrochemical [21] and fluorescence [22]. We expect that the aptasensor operated with a wide calibration curve and low LOD can be applied for a more accurate identification of blood clots.

As shown in Fig. 6, The relative CL intensity in the presence of thrombin was enhanced, whereas the relative CL intensities in the
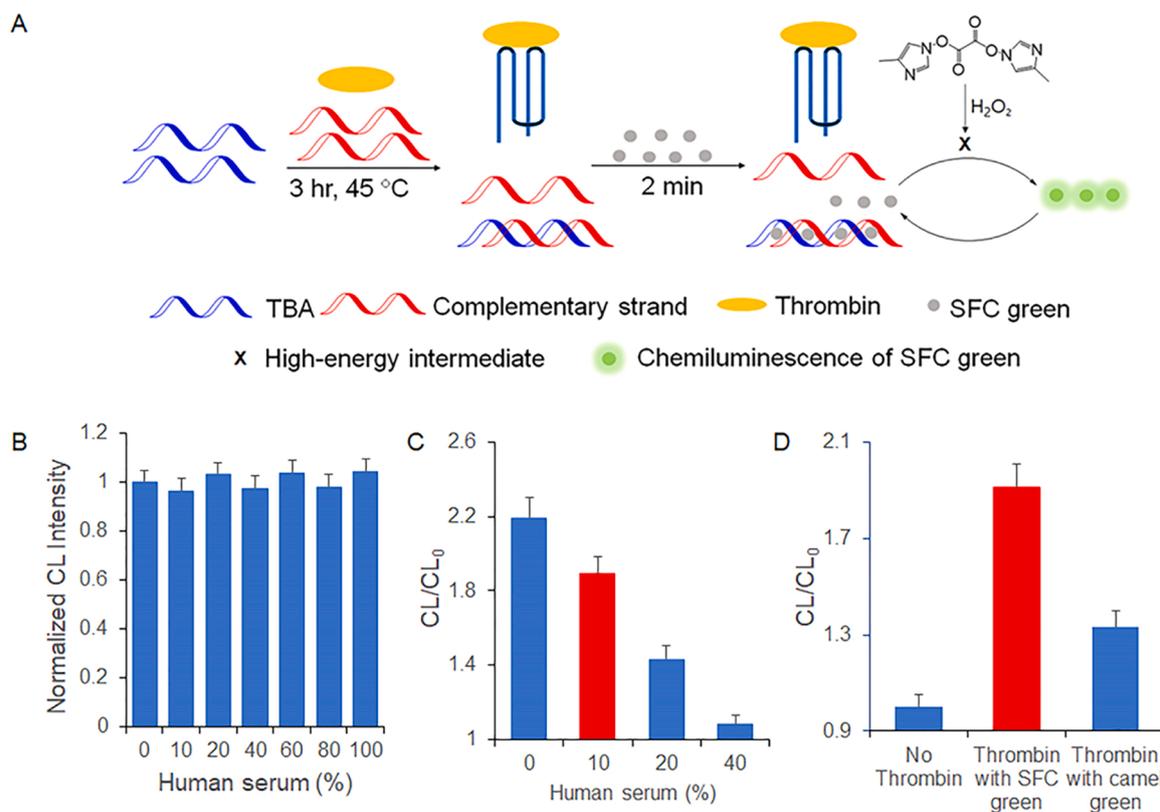
Fig. 5. . (A) Operation method of the competitive aptasensor, (B) ODI-CL emission of SFC green in the absence and presence of human serum, (C) CL/CL_0 of the competitive aptasensor in the absence and presence of human serum, (D) CL/CL_0 of SFC (or camel) green in the absence and presence of thrombin (300 mU/ml) in a sample containing 10 % human serum.

Table 1

Comparison of the current and other biosensors for the quantification of thrombin.

Method	Sample	Dynamic range (nM)	LOD (pM)	Ref.
Lateral Flow Assay with a colorimetric detection	Serum	20–260	3000	[20]
Magnetic force assisted electrochemical sensor	Serum	1.0–500	490	[21]
Electrochemiluminescence platform	Serum	0.0001–10	0.029	[22]
Protein-induced fluorescence	Plasma	0.25–25	8.9	[23]
Luminol chemiluminescence	Serum	1–25	83	[24]
Competitive aptasensor with an ODI-CL detection	Serum	0.14 – 4.61	43	This research
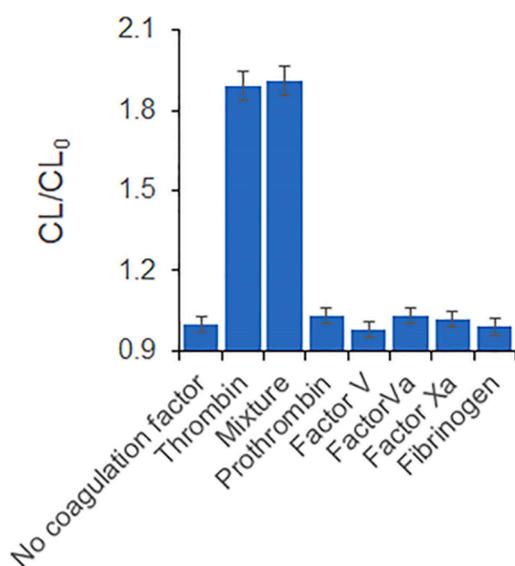
Fig. 6. Selectivity of the biosensor capable of sensing thrombin, [thrombin] = 15 ng/ml (300 mU/ml), [other factors] = 50 ng/ml.

presence of other coagulation factors was the same as CL_0 in the absence of any coagulation factor within an acceptable statistical error range (± 5 %). The results indicate that the competitive aptasensor can quantified thrombin in 10 % human serum with good selectivity.

Table 2 shows that the competitive aptasensor with ODI-CL detection can quantify thrombin in 10 % human serum with good accuracy, precision, and recovery. The accuracy range of the biosensor was 4 – 12.5 %. The precision range of the biosensor was 3.8 – 6.7 %. In addition, the recovery range of the biosensor was 95 – 112.5 %.

The good correlation between the competitive aptasensor and the protease enzyme analysis shown in Table 3 indicate that the competitive aptasensor can be applied as a new analytical method capable of rapidly quantifying and monitoring thrombin in 10 % human sample.

4. Conclusions

A highly selective and sensitive competitive aptasensor with ODI-CL detection, capable of quantifying trace levels of thrombin in 10 % human serum, was developed using the combination of thrombin, TBA, and the complementary strand of TBA. We confirmed that the competitive aptasensor was able to be developed because the formation of G-quadruplex from the binding interaction of thrombin and TBA is faster than the hybridization of TBA and the complementary strand. Thus, CL emission of SFC (or camel) green was proportionally enhanced with the increase of thrombin in a sample due to the increase of G-quadruplex concentration and reduction of dsDNA concentration. We expect the

Table 2

Accuracy, precision, and recovery of the biosensor with ODI-CL detection (N = 5).

Sample	Spiked (mU/ml)	Detected (mU/ml)	Recovery (%)
1	40	45 ± 3	112.5
2	80	76 ± 5	95.0
3	300	312 ± 12	104.0

Table 3

Correlation between the competitive aptasensor and protease enzyme analysis using a fluorogenic substrate for the quantification of thrombin in samples containing 10 % human serum (N = 3).

Sample	Competitive aptasensor (mU/ml)	Protease enzyme analysis (mU/ml)
1	87 (± 6.5)	92 (± 4.7)
2	127 (± 5.5)	134 (± 6.7)
3	195 (± 7.2)	191 (± 8.1)
4	258 (± 10.8)	266 (± 9.3)
5	338 (± 13.6)	332 (± 11.1)

label and washing free aptasensor can be cost-effectively applied for the accurate monitoring of blood clots occurring with severe COVID-19 infection.

It is expected that the concept and principle derived from results confirmed in this research can be applied for the development of various biosensors capable of early diagnosing human diseases and rapidly monitoring toxic materials existing in food and nature. This is because various DNA aptamers, capable of binding biomarkers and toxic materials with good selectivity, have been designed and synthesized [25–27]. In conclusion, the competitive aptasensor with ODI-CL detection designed based on the new technology can be applied in various fields such as analytical chemistry, biology, biomedical engineering, clinical science, environmental engineering, food safety, pharmacology, and toxicology.

CRediT authorship contribution statement

Jaden Yun: Conceptualization, Methodology, Validation, Data curation, Investigation, Writing – original draft. **Ji Hoon Lee**: Conceptualization, Methodology, Writing – review & editing, Supervision.

Declaration of Competing Interest

The authors declare that they have no known competing financial interests or personal relationships that could have appeared to influence the work reported in this paper.

Data Availability

No data was used for the research described in the article.

Acknowledgements

Appendix A. Supporting information

Supplementary data associated with this article can be found in the online version at doi:10.1016/j.jpba.2022.115076.

References

[1] J.A. Stefely, B.B. Christensen, T. Gogakos, J.K.C. Sullivan, G.G. Montgomery, J. P. Barranco, E.M. Van Cott, Marked factor V activity elevation in severeCOVID-19

is associated with venous thromboembolism, Am. J. Hematol. 95 (12) (2020) 1522–1530.

[2] R. Gupta, M. Majumdar, R. Imran, J. Yi, A comprehensive review on antithrombotic therapy for peripheral artery disease, Semin. Vasc. Surg. 35 (2) (2022) 124–131.

[3] M.R. Montinari, S. Minelli, From ancient leech to direct thrombin inhibitors and beyond: new from old, Biomed. Pharmacother. 149 (2022), 112878.

[4] C. Tuerk, L. Gold, Systematic evolution of ligands by exponential enrichment - RNA ligands to bacteriophage-T4 DNA-polymerase, Science 249 (4968) (1990) 505–510.

[5] A.D. Ellington, J.W. Szostak, Invitro selection of RNA molecules that bind specific ligands, Nature 346 (6287) (1990) 818–822.

[6] L.C. Bock, L.C. Griffin, J.A. Latham, E.H. Vermaas, J.J. Toole, Selection of single-stranded-DNA molecules that bind and inhibit human thrombin, Nature 355 (6360) (1992) 564–566.

[7] S. Cho, L. Park, R. Chong, Y.T. Kim, J.H. Lee, Rapid and simple G-quadruplex DNA aptasensor with guanine chemiluminescence detection, Biosens. Bioelectron. 52 (2014) 310–316.

[8] K. Shao, B.R. Wang, S.Y. Ye, Y.P. Zuo, L. Wu, Q. Li, Z.C. Lu, X.C. Tan, H.Y. Han, Signal -Amplified near -infrared ratiometric electrochemiluminescence aptasensor based on multiple quenching and enhancement effect of graphene/gold nanorods/ G-Quadruplex, Anal. Chem. 88 (16) (2016) 8179–8187.

[9] R.F. Macaya, P. Schultze, F.W. Smith, J.A. Roe, J. Feigon, Thrombin-binding DNA aptamer forms a unimolecular quadruplex structure in solution, Proc. Natl. Acad. Sci. USA 90 (8) (1993) 3745–3749.

[10] J.H. Lee, J.C. Rock, S.B. Park, M.A. Schlautman, E.R. Carraway, Study of the characteristics of three high-energy intermediates generated in peroxyoxalate chemiluminescence (PO-CL) reactions, J. Chem. Soc. -Perkin Trans. 2 (4) (2002) 802–809.

[11] J.H. Lee, J. Je, M.A. Schlautman, E.R. Carraway, Fast peroxyoxalate chemiluminescence for minimized analytical separation systems, Chem. Commun. (2003) 270–271.

[12] P.S. Park, T.H.D. Rho, Y.T. Kim, S.O. Ko, M.A. Schlautman, E.R. Carraway, J. H. Lee, Evidence of multiple pathways capable of emitting peroxyoxalate chemiluminescence using a charge coupled device spectrometer, Chem. Commun. 47 (19) (2011) 5542–5544.

[13] J. Choi, Y.T. Kim, J.H. Lee, Rapid quantification of melamine in milk using competitive 1,1 ′-oxalyldiimidazole chemiluminescent enzyme immunoassay, Analyst 135 (9) (2010) 2445–2450.

[14] J.H. Lee, J.E.R. Rho, T.H.D. Rho, J.G. Newby, Advent of innovative chemiluminescent enzyme immunoassay, Biosens. Bioelectron. 26 (2) (2010) 377–382.

[15] J. Kwun, S. Yun, L. Park, J.H. Lee, Development of 1,1 ′-oxalyldiimidazole chemiluminescent biosensor using the combination of graphene oxide and hairpin aptamer and its application, Talanta 119 (2014) 262–267.

[16] H. Khang, J. Cho, S. Chong, J.H. Lee, All-in-one dual-aptasensor capable of rapidly quantifying carcinoembryonic antigen, Biosens. Bioelectron. 90 (2017) 46–52.

[17] A. Karsai, S. Muller, S. Platz, M.T. Hauser, Evaluation of a homemade SYBR (R) Green I reaction mixture for real-time PCR quantification of gene expression, Biotechniques 32 (4) (2002) 790–796.

[18] S.N. Hu, X.W. Liu, Y. Gao, R.F. Zhou, M.Y. Wei, J. Dong, H.L. Yan, Y.R. Zhao, Hepatitis B virus inhibits neutrophil extracellular trap release by modulating reactive oxygen species production and autophagy, J. Immunol. 202 (3) (2019) 805–815.

[19] E. Graugnard, A. Cox, J. Lee, C. Jorcyk, B. Yurke, W.L. Hughes, Kinetics of DNA and RNA hybridization in serum and serum-SDS, IEEE Trans. Nanotechnol. 9 (5) (2010) 603–609.

[20] M. Mahmoud, C. Ruppert, S. Rentschler, S. Laufer, H.P. Deigner, Combining aptamers and antibodies: Lateral flow quantification for thrombin and interleukin-6 with smartphone readout, Sens. Actuator B-Chem. 333 (2021), 129246.

[21] S. Chung, J.M. Moon, J. Choi, H. Hwang, Y.B. Shim, Magnetic force assisted electrochemical sensor for the detection of thrombin with aptamer-antibody sandwich formation, Biosens. Bioelectron. 117 (2018) 480–486.

[22] C.N. Yang, Y. Tian, B.Y. Wang, Q.F. Guo, G.M. Nie, "Signal-on" molecularly imprinting-aptamer electrochemiluminescence platform for ultrasensitive detection of thrombin, Sens. Actuator B-Chem. 338 (2021), 129870.

[23] S. Umrao, V. Jain, Anusha, B. Chakraborty, R. Roy, Protein-induced fluorescence enhancement as aptamer sensing mechanism for thrombin detection, Sens. Actuator B-Chem. 267 (2018) 294–301.

[24] Y.N. Lin, J.B. Li, Y.H. Wang, Y.L. Sun, C.F. Ding, W.Y. Sun, C.N. Luo, A chemiluminescence biosensor for the detection of thrombin based on the aptamer composites, Spectrochim. Acta Part a-Mol. Biomol. Spectrosc. 192 (2018) 153–158.

[25] K. Mao, H. Zhang, Y.W. Pan, K.K. Zhang, H.R. Cao, X.Q. Li, Z.G. Yang, Nanomaterial-based aptamer sensors for analysis of illicit drugs and evaluation of drugs consumption for wastewater-based epidemiology, Trac-Trends Anal. Chem. 130 (2020), 115975.

[26] L.Y. Yang, T. Gao, W.J. Li, Y. Luo, S. Ullah, X.N. Fang, Y.W. Cao, R.J. Pei, Ni-Nitrilotriacetic acid affinity SELEX Method for Selection of DNA aptamers specific to the N-cadherin protein, ACS Comb. Sci. 22 (12) (2020) 867–872.

[27] E.M. McConnell, J. Nguyen, Y.F. Li, Aptamer-based biosensors for environmental monitoring, Front. Chem. 8 (2020) 434.